MOLECULAR AND CELLULAR BIOLOGY, Mar. 2010, p. 1116–1129 Vol. 30, No. 5
0270-7306/10/$12.00 doi:10.1128/MCB.01229-09

Asf1 Can Promote Trimethylation of H3 K36 by Set2▽

Ling-ju Lin,[1] Laura V. Minard,[1] Gerald C. Johnston,[2] Richard A. Singer,[3] and Michael C. Schultz[1]*

Department of Biochemistry, University of Alberta, Edmonton, Alberta, Canada T6G 2H7,[1] and Department of Microbiology and Immunology[2] and Department of Biochemistry and Molecular Biology,[3] Dalhousie University, Halifax, Nova Scotia, Canada B3H 1X5

Received 11 September 2009/Returned for modification 20 October 2009/Accepted 22 December 2009

Asf1 is a conserved histone H3/H4 chaperone that can assemble and disassemble nucleosomes and promote histone acetylation. Set2 is an H3 K36 methyltransferase. The functions of these proteins intersect in the context of transcription elongation by RNA polymerase II: both contribute to the establishment of repressive chromatin structures that inhibit spurious intragenic transcription. Here we characterize further interactions between budding yeast (*Saccharomyces cerevisiae*) Asf1 and Set2 using assays of intragenic transcription, H3/H4 posttranslational modification, coding region cross-linking of Asf1 and Set2, and cooccurrence of Asf1 and Set2 in protein complexes. We find that at some genes Asf1 and Set2 control chromatin metabolism as components of separate pathways. However, the existence of a low-abundance complex containing both proteins suggests that Asf1 and Set2 can more directly collaborate in chromatin regulation. Consistent with this possibility, we show that Asf1 stimulates Set2 occupancy of the coding region of a highly transcribed gene by a mechanism that depends on Asf1 binding to H3/H4. This function of Asf1 promotes the switch from di- to trimethylation of H3 K36 at that gene. These results support the view that Set2 function in chromatin metabolism can intimately involve histone chaperone Asf1.

Transcriptional regulation in eukaryotes critically involves the regulation of histone-DNA complexes. Two conserved proteins that modulate the properties of histone-DNA complexes in budding yeast (*Saccharomyces cerevisiae*) are Asf1 and Set2. Asf1 and Set2 have quite distinct biochemical activities. Asf1 is a histone chaperone that binds tightly to the dimer formed by histones H3 and H4 (13, 35). It can deposit H3/H4 onto DNA and remove H3/H4 from nucleosome core particles (35, 44). Asf1 also modulates the enzymatic activity of some histone-directed lysine acetylases (KATs). It stimulates Rtt109 acetylation of H3 K56 (10, 20) by a mechanism that requires Asf1 binding to H3/H4 (21). Asf1 can also inhibit acetylation: this activity has been reported in the context of H3/H4 acetylation by the SAS complex (49). In contrast to Asf1, Set2 is an enzyme. It catalyzes mono-, di-, and trimethylation of H3 K36 in nucleosome core particles (11, 16, 47).

Since Asf1 and Set2 regulate the properties of histone-DNA complexes and these properties affect all steps in the transcription cycle of nuclear genes, it is not surprising that Asf1 and Set2 have both been implicated in the control of transcriptional activation, initiation, and elongation by RNA polymerase II (RNAP II). These regulatory functions of Asf1 and Set2 are best understood in budding yeast. Asf1 potentiates early steps in the transcription cycle by stimulating H3 K56 acetylation, which destabilizes nucleosomes and makes them easier to evict (55). Set2 somehow modulates promoter binding by TATA binding protein (TBP) and transcription factor IIA (TFIIA), although the precise mechanism remains unknown (4). As far as we are aware, there is no evidence that Asf1 and Set2 function in the same pathway of nucleosome metabolism in promoters and *cis*-acting control regions.

The critical function of Asf1 during transcription elongation is to disassemble nucleosomes ahead of elongating RNAP II and reassemble them behind it (42). By virtue of these two activities, Asf1 promotes elongation and reestablishes a chromatin architecture that disfavors spurious initiation within coding regions.

In contrast, Set2 has a single known function in coding regions: it inhibits elongation by catalyzing methylation of H3 K36. Although Set2 catalyzes mono-, di-, and trimethylation of H3 K36, dimethylation is fully sufficient for inhibition of elongation by Set2 (32, 59). This inhibition is a stepwise process. First, Set2 dimethylates K36 of nucleosomal H3. Second, the Rpd3S histone deacetylase (HDAC) complex binds to H3 K36-methylated nucleosomes (6, 31). Third, deacetylation of nucleosomes by Rpd3S makes chromatin less permissive for elongation by RNAP II. Both Asf1 and Set2 can modulate the properties of chromatin in a way that inhibits transcription during elongation. By virtue of this activity, both proteins are able to dampen spurious transcription from cryptic promoters in coding regions (7, 42). Whether Asf1 and Set2 can collaborate in this regulation, either as part of the same pathway or converging pathways, remains unknown.

The regulation of Set2-dependent H3 K36 trimethylation is just beginning to be understood. The available evidence suggests that H3 K36 trimethylation of chromatin is directly coupled to transcriptional elongation, since it requires the following: (i) the C-terminal domain (CTD) of RNAP II, (ii) an enzyme that phosphorylates the CTD during elongation (Ctk1), and (iii) a domain in Set2 that interacts with the CTD (59). Set2 binding to H4 (11) and rotation of H3 around proline 38 (36, 59) are also important for H3 K36 trimethylation.

In this report, we further examine the functions of Asf1 and Set2 in the coding regions of active genes. Our results suggest

* Corresponding author. Mailing address: Department of Biochemistry, University of Alberta, MSB 5-76, Edmonton, Alberta, Canada T6G 2H7. Phone: (780) 492-9144. Fax: (780) 492-9556. E-mail: michael.schultz@ualberta.ca.

▽ Published ahead of print on 4 January 2010.

that Asf1 can function separately from Set2 in chromatin regulation during elongation or directly modulate the activity of Set2.

MATERIALS AND METHODS

Strains and media. Except as noted under "Synthetic genetic analysis" below, all strains used are derived from *S. cerevisiae* BY4741 (*MAT***a** *his3Δ1 leuΔ0 met15Δ0 ura3Δ0*) (5). Chromosomal mutations were generated by one-step integration using PCR products obtained from previously described plasmids (18, 33, 45). The addition of sequences encoding the myc and hemagglutinin (HA) epitope tags was verified by PCR using three primer sets (flanking the target gene, internal to the target gene, and flanking primer plus primer specific for the marker; sequences available upon request). The *asf1*Δ::*kanMX*, *set2*Δ::*kanMX*, *eaf3*Δ::*kanMX*, and *rtt109*Δ::*kanMX* deletion mutants from the *S. cerevisiae* haploid nonessential gene deletion library (56) were verified to be correct by PCR. The *asf1*Δ::*kanMX set2*Δ::*nat*^{r}, *asf1*Δ::*kanMX rpd3*Δ::*HIS3MX6*, *asf1*Δ::*nat*^{r} *eaf3*Δ::*kanMX*, *asf1*Δ:: *kanMX sds3*Δ:: *nat*^{r}, and *rtt109*Δ::*kanMX set2*Δ::*nat*^{r} double mutants were used. The *rpd3*Δ::*HIS3MX6* and *sds3*Δ:: *nat*^{r} deletion mutants were constructed by R. Friis in the laboratory of M. C. Schultz. The strains expressing Set2-TAP and Asf1-TAP are described by Ghaemmaghami et al. in reference 17. pRS314-based and pRS316-based plasmids harboring *ASF1* and *asf1*^{V94R} (34) were transformed into an *asf1Δ set2*Δ strain for Northern blotting analysis and into a *SET2-TAP asf1*Δ strain for chromatin immunoprecipitation (ChIP) analysis. A strain expressing HA-tagged Asf1^{V94R} (Asf1^{V94R}-HA) from its normal chromosomal location was constructed in multiple steps by H. Mewhort. Briefly, the *asf1*^{V94R} mutation was created using site-directed mutagenesis and propagated as an EcoRI/XhoI insert in pGEX6P-1. The correct GT → CG mutation at 280 bp of *ASF1* was confirmed by sequencing. A cassette containing (i) *asf1*^{V94R} with sequence encoding the 3HA epitope tag at its 3′ end and (ii) the *kanMX* G418 resistance marker was then assembled in *Escherichia coli* plasmid pHM3. PCR was used to amplify this cassette and appropriate targeting sequences up- and downstream of the *ASF1* open reading frame (ORF). The PCR product was transformed into *S. cerevisiae* BY4741. Successful incorporation of both the V94R mutation and the 3HA epitope was confirmed by genomic sequencing and immunoblotting, respectively. Further details are available on request. All media were prepared as described previously, and standard genetic methods for mating, sporulation, transformation, and random spore analysis were used throughout this study (53). For testing sensitivity to 6-azauracil (6-AU), strains were transformed to Ura$^+$ (40) using plasmid pRS316 (45). They were spotted onto medium lacking uracil and containing 25 to 100 μg of 6-AU per ml. Sensitivity to hydroxyurea (HU) and methane methylsulfonate (MMS) was tested by spotting strains onto medium containing 50 and 100 mM HU and 0.005 and 0.01% MMS.

Synthetic genetic analysis. Automated synthetic genetic analysis (SGA) was performed by the method of Tong et al. (52) using an *asf1*Δ query strain (Y2454 background) and the yeast haploid gene deletion collection. To generate the query strain, *ASF1* was replaced with a nourseothricin resistance cassette (18) in strain Y2454 (*MAT*α *mfa1*Δ::*MFA1pr-HIS3 can1Δ ura3Δ0 leu2Δ0 his3Δ1 lys2Δ0*) using homologous recombination. Oligonucleotides bearing sequences flanking the *ASF1* coding region and plasmid pAG25 as a template (52) were used to generate the deletion cassette by PCR amplification. Correct replacement of *ASF1* was verified by PCR analysis.

Flow cytometry. Cellular DNA content was determined by flow cytometry as described previously (39). Briefly, cells were stained with propidium iodide, sonicated, and analyzed using a FACScan flow cytometer (Becton-Dickinson).

Immunoblotting. Total proteins were prepared by trichloroacetic acid precipitation (39). Identical cell equivalents of protein in samples were compared. Antibodies that recognize total histone H3 (ab1791), monomethylated histone H3 K36 (ab9048), and trimethylated histone H3 K36 (ab9050) were obtained from Abcam, and antibodies that recognize calmodulin binding protein (CBP) (07-482), dimethylated histone H3 K36 (07-369), acetylated H3 K9 (07-352), acetylated H3 K14 (07-353), and tetra-acetylated H4 (06-866) were obtained from Upstate. The antibody against actin (MAB 1501) was obtained from Millipore. The 12CA5 antibody for detecting the HA epitope was from Roche. Quantitative analysis of total H3 trimethylated K36 (K36me3) was performed using ImageJ 1.38x after optical scanning of appropriately exposed films. H3 K36me3 signals were normalized to bulk H3 recovery, which was assessed by analysis of blots probed with the total histone H3 antibody (ab1791).

Chromatin immunoprecipitation (ChIP). Yeast strains were grown at 30°C in yeast extract-peptone-dextrose (YPD) to a concentration of 1×10^7 cells per ml. Chromatin immunoprecipitation was performed essentially as described previously (3), using antibodies that recognize the myc tag (9E10) or total H3 (ab1791) or are specific for dimethylated H3 K36, trimethylated K9/K14 acetylated H3 (06-599; Upstate), tetra-acetylated H4 (K5, K8, K12, and K16), or K16 acetylated H4 (07-329; Upstate). Set2-TAP was recovered from sonicates using IgG-Sepharose 6 Fast Flow (17-0969-01; GE) based on the IgG-agarose protocol in reference 28. Immunoprecipitation was performed overnight at 4°C. Input and immunoprecipitated DNA was purified using Qiagen PCR purification columns and analyzed by standard PCRs to which 1 μCi of ^{32}P-labeled dCTP had been added. Primers used for ChIP assays are described in reference 8. A region proximal to the telomere of chromosome 5 (TELV) was used as a control (8). PCR signals were captured using a Storm 840 phosphorimager and quantified using ImageQuant software (Molecular Dynamics). For localization of Set2-TAP, Asf1-myc, and H3, ChIP was quantified by normalizing band intensities for each sample using the following calculation as described in reference 6: (specific gene IP/TELV IP)/(specific gene input/TELV input). The normalized ChIP value calculated for H3 dimethylated K36 (K36me2), H3 K36me3, H3 acetylated K9 or acetylated K14 (K9ac/K14ac), or acetylated H4, was divided by the normalized ChIP value calculated for total H3. Statistical significance was assessed by applying Student's unpaired (independent) two-tailed *t* test for three independent samples of each strain under consideration.

Tandem affinity purification and protein identification by mass spectrometry. Tandem affinity purification of protein complexes was performed using extracts from the indicated strains essentially as described previously (27). Proteins stained with Sypro Ruby (Invitrogen) were in-gel digested with trypsin. Spectra were obtained by matrix-assisted laser desorption ionization–time of flight (MALDI-ToF) mass spectrometry and analyzed using Mascot software in the Institute for Biomolecular Design at the University of Alberta.

RNA isolation and Northern blotting analysis. Total RNA was isolated by hot phenol extraction (14) from cells grown in YPD to a concentration of 1×10^7 cells per ml. DNA probes were prepared by random primed labeling of PCR products for *FLO8* (+1672/+2399), *SPB4* (+1100/+1820), *ACT1*, and *SCR1*.

RESULTS

Genetic interactions between *ASF1* and *SET2*. In a high-throughput genetic screen, we uncovered a synthetic sick interaction between *ASF1* and *SET2*, which was confirmed by random spore analysis (Fig. 1A) (this interaction has been reported by others [9]). We also found that an *asf1*Δ *set2*Δ strain generated by successive one-step gene replacements grows at a much lower rate than either single mutant at 30°C and that this phenotype is slightly exacerbated at 37°C (Fig. 1B). These results prompted us to examine in more detail the nature of functional interactions between Asf1 and Set2.

We used flow cytometry to assess the impact of individual and combined deletion of *ASF1* and *SET2* on cell cycle progression (Fig. 1C). Consistent with previous work (54), we find that *asf1*Δ cells accumulate with a G_2/M content of DNA and take longer than wild-type cells to complete S phase. In contrast, the flow cytometry profile of *set2*Δ cells is very similar to the profile of wild-type cells. Furthermore, the cell cycle profile of the *asf1*Δ mutant is unaffected by deletion of *SET2*. Therefore, Asf1 and Set2 do not perform the same function in parallel pathways of chromatin regulation that affect cell cycle progression under normal culture conditions.

Because the regulation of chromatin structure is important for protection from DNA damage, we tested whether Asf1 and Set2 both function in pathways that protect cells from DNA structure abnormalities. As previously reported (54), loss of *ASF1* enhances the sensitivity of yeast to two genotoxins, hydroxyurea (HU) and methane methylsulfonate (MMS) (Fig. 2A and B). *SET2* null mutants, on the other hand, grow similarly to wild-type cells in the presence of these agents. Furthermore, the sensitivity of the *asf1*Δ *set2*Δ double mutant to HU and MMS is only marginally greater than that of the *asf1*Δ

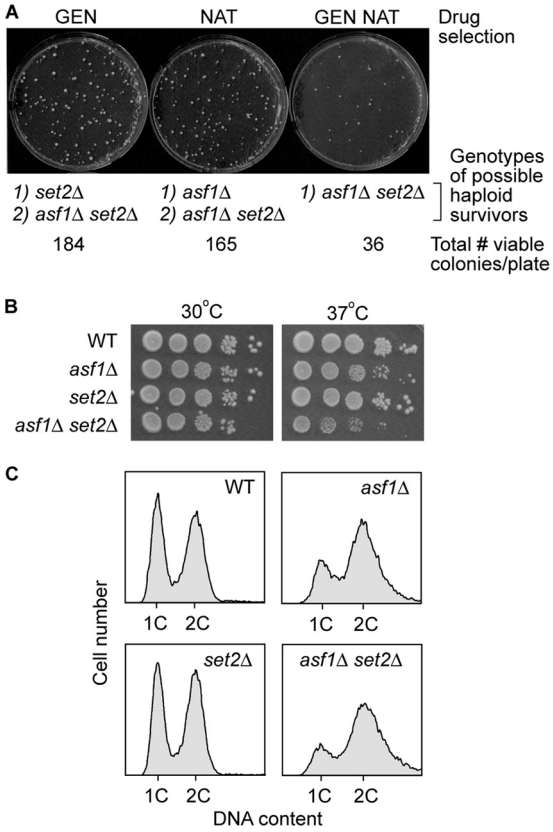

FIG. 1. Genetic interactions between *ASF1* and *SET2*. (A) Random spore analysis was performed on *ASF1*/*asf1*Δ::*NAT SET2*/*set2*Δ::*GEN* diploids generated by synthetic genetic array methodology. Diploids were grown in liquid sporulation medium and plated onto haploid-specific solid medium containing Geneticin (GEN), nourseothricin (NAT), or both GEN and NAT. The plates were photographed after 4 days of growth at 30°C. (B) Simultaneous deletion of *ASF1* and *SET2* confers a synthetic sick phenotype. Fivefold serial dilutions of cells were spotted onto YPD plates and photographed after 3 days of growth at 30 and 37°C. (C) The DNA content of asynchronous cultures of wild-type (WT), *asf1*Δ, *set2*Δ, and *asf1*Δ *set2*Δ strains was determined by flow cytometry analysis.

single mutant. Therefore, Set2 is probably not in a major Asf1-dependent pathway of chromatin metabolism that protects cells from genotoxin-induced DNA structure abnormalities. This conclusion is supported by the observations that *set2*Δ cells are more sensitive to UV irradiation than *asf1*Δ cells are and that the *asf1*Δ *set2*Δ double mutant is no more sensitive to UV than the *set2*Δ single mutant is (Fig. 2C).

Like wild-type cells, *SET2* null mutants arrest in early S phase when treated with 0.2 M HU or 0.1% MMS (Fig. 2D and E). Despite the fact that they progress slowly through the division cycle, *asf1*Δ cells also arrest predominantly in early S phase in response to HU and MMS. The response of *asf1*Δ *set2*Δ cells to HU and MMS is identical to the response of *asf1*Δ cells. Therefore, Asf1 and Set2 do not have similar functions in the control of cell cycle progression under environmental conditions that cause DNA structure abnormalities. Collectively, these results suggest that Asf1 and Set2 do not have similar core functions in steps of chromatin regulation that affect cell cycle progression or DNA structure checkpoint responses.

Since Asf1 and Set2 are known to function in steps of chromatin regulation that are coupled to elongation by RNAP II (see the introduction), we predicted that they might share phenotypes connected to misregulation of this phase of the transcription cycle. One such phenotype of *set2*Δ cells is resistance to the elongation inhibitor 6-azauracil (6-AU) (24, 26). We therefore tested the effect of 6-AU on *set2*Δ and *asf1*Δ cells in a side-by-side spotting experiment (Fig. 2F). As expected (24, 26), *set2*Δ cells exhibited increased resistance to 6-AU compared to wild-type cells. Surprisingly, however, *asf1*Δ cells are hypersensitive to 6-AU. Compared to the single mutants, *asf1*Δ *set2*Δ cells have intermediate sensitivity to 6-AU. On the basis of these results, we consider it unlikely that Asf1 and Set2 have similar global roles in the regulation of RNAP II transcription.

H3 tail acetylation and K36 methylation are misregulated in *ASF1* and *SET2* null mutants. Both Asf1 and Set2 contribute to the regulation of acetylation of the core histones. Asf1 promotes acetylation of H3 at K56 by stimulating the KAT activity of Rtt109 (10, 20). Set2 promotes deacetylation of H3 and H4 by a mechanism that affects histone deacetylase (HDAC) recruitment to chromatin (reviewed in reference 46). In other words, Asf1 and Set2 have opposite effects on H3 acetylation. Accordingly, we predicted that the combined effect of deleting *ASF1* and *SET2* on overall H3 K9 and K14 acetylation would be intermediate between the effects of the individual deletions.

To test this prediction, we analyzed total protein extracts from wild-type, *asf1*Δ, *set2*Δ, and *asf1*Δ *set2*Δ strains by immunoblotting, using antibodies that specifically detect K9- and K14-acetylated H3 (Fig. 3A). As previously reported (1, 2), overall acetylation of H3 at these sites is lower in *asf1*Δ cells than in wild-type cells. In *set2*Δ cells, H3 K9/K14 acetylation is elevated. The overall H3 acetylation phenotype of the *asf1*Δ *set2*Δ double mutant falls between that of the single mutants (higher than the *asf1*Δ mutant but lower than the *set2*Δ mutant). Therefore, on a global scale, the effects of *ASF1* and *SET2* deletion on H3 tail acetylation seem to offset one another.

We next turned our attention to the control of histone methylation as a possible node at which the functions of Asf1 and Set2 intersect. By immunoblotting, Cheung et al. observed no effect of deletion of *ASF1* on overall H3 K36 methylation (7). Our results are not as clear-cut. That is, while H3 monomethylated K36 (K36me1) and H3 K36me2 were unaffected by *ASF1* deletion, in 7 of 10 independent comparisons between log-phase wild-type and *asf1*Δ cells, H3 K36me3 was reduced in the mutant (Fig. 3B shows a representative example). Because three comparisons suggested equivalent H3 K36me3 expression in wild-type and *asf1*Δ cells, the experiment was repeated by analyzing total protein obtained in parallel from four independent wild-type cultures and four independent null mutant cultures. H3 K36me3 and total H3 expression were assayed by immunoblotting and quantitated. The results, in Fig. 3C, support the conclusion that deletion of *ASF1* is associated with lower overall H3 K36 trimethylation. Since Set2 protein levels are the same in wild-type and *asf1*Δ cells (Fig. 3D), this phenotype does not reflect Asf1 regulation of steady-state Set2

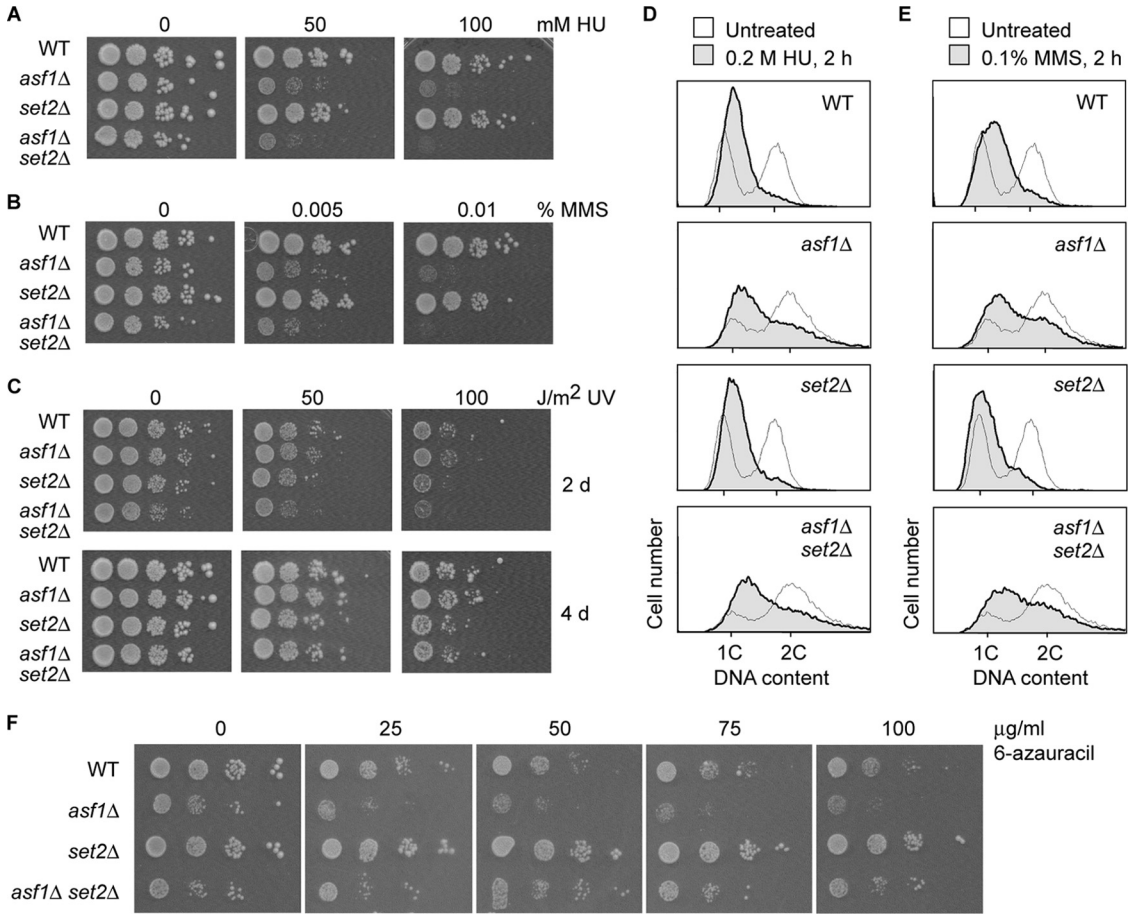

FIG. 2. Sensitivity of *ASF1* and *SET2* null mutants to DNA damaging agents and 6-azauracil. (A to C) Serial dilutions of cells were spotted onto YPD plates containing the indicated concentrations of hydroxyurea (HU) and methane methylsulfonate (MMS) or spotted onto YPD and then UV irradiated. The plates were photographed after growth at 30°C (3 days in panels A and B and 2 or 4 days in panel C). (D and E) DNA content of cultures of wild-type, *asf1*Δ, *set2*Δ, and *asf1*Δ *set2*Δ strains that were left untreated or exposed to the indicated concentrations of HU or MMS for 2 h. The flow cytometry profiles of untreated (asynchronous) cultures are shaded; the dotted lines are the profiles of the treated cultures. (F) *ASF1* and *SET2* null mutants have opposite responses to the transcription elongation inhibitor 6-azauracil. Log-phase cells of the indicated strains were spotted in 10-fold serial dilutions onto plates containing increasing amounts of 6-azauracil. The plates were photographed following 4 days of growth at 30°C.

expression. These findings led us to further explore the possibility that Asf1 does modulate methylation of H3 K36.

Separate Asf1- and Set2-dependent pathways for suppression of spurious intragenic transcription. H3 K36 methylation by Set2 plays an important role in the suppression of spurious transcription within the coding regions of genes. Specifically, chromatin deacetylation which inhibits spurious transcription depends on binding of the Rpd3S HDAC complex to nucleosomes that have been dimethylated at H3 K36 by Set2 (46).

Asf1 also inhibits spurious transcription within coding regions (7, 42), raising the possibility that it functions in the Set2-dependent pathway of elongation-coupled chromatin remodeling. We tested this possibility by several approaches. First, we used Northern blotting to compare the effects of individual and combined deletions of *ASF1* and *SET2* on spurious intragenic transcription at *FLO8*.

In some chromatin metabolism mutants which cannot fully suppress spurious transcription within coding regions, two novel *FLO8* transcripts have been detected: the major abnormal transcript produced by conditional *SPT6* mutants under restrictive conditions (23) likely corresponds to the "short" transcript in Fig. 4A, while the slower-migrating spurious transcript previously observed in *set2*Δ cells (6) likely corresponds to the "long" transcript. As expected (6), a long intragenic *FLO8* transcript is induced in cells lacking Set2 (Fig. 4A). Under the conditions used here, we observe little or no induction of these species when *ASF1* is deleted (Fig. 4A and C to E). Therefore, if Asf1 functions at *FLO8* in a Set2-dependent pathway for suppression of spurious intragenic transcription, it is not an essential component of this pathway.

The notion that Asf1 is not necessary for Set2-dependent inhibition of spurious intragenic transcription at *FLO8* is supported by the finding that combined deletion of both *ASF1* and *SET2* is associated with strong induction of the short intragenic transcript and modest induction of the long transcript. It is apparent from the result for the double mutant (Fig. 4A) that Asf1 can contribute to inhibition of spurious intragenic transcription in *FLO8* by a mechanism that does not require H3

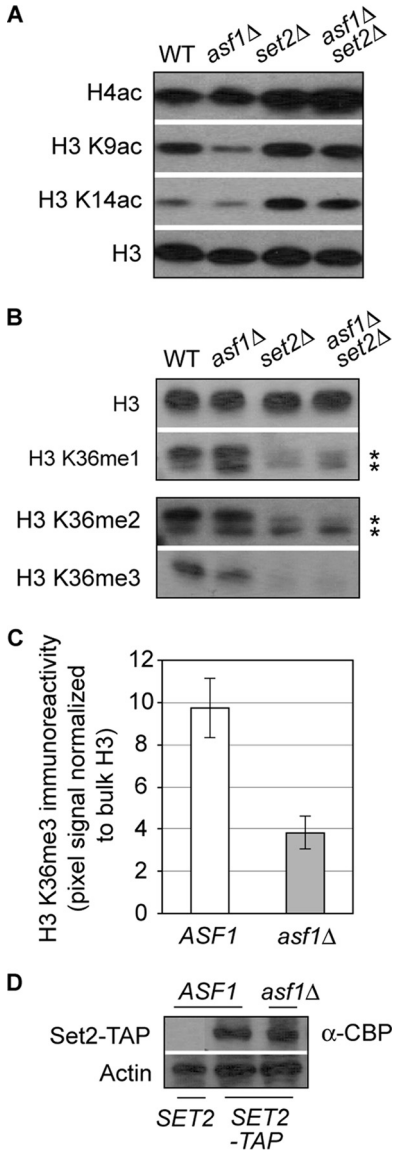

FIG. 3. Asf1 and Set2 influence global histone H3/H4 tail acetylation and H3 K36 methylation. Immunoblots of total protein from wild-type and mutant strains were probed using the indicated site-specific antibodies. "H4ac" is H4 acetylated at one or more of K5, K8, K12, and K16 in its amino-terminal tail. In panels A and B, equal loading was confirmed by analysis of total H3. (C) Quantitative analysis of overall H3 K36me3 expression in wild-type and *asf1*Δ cells. The signal for H3 K36me3 was normalized to the amount of total H3. (D) Effect of *ASF1* deletion on Set2 expression. The immunoblot shows the level of TAP-tagged Set2 in wild-type and *asf1*Δ strains. Actin is the loading control. α-CBP, anti-CBP antibody.

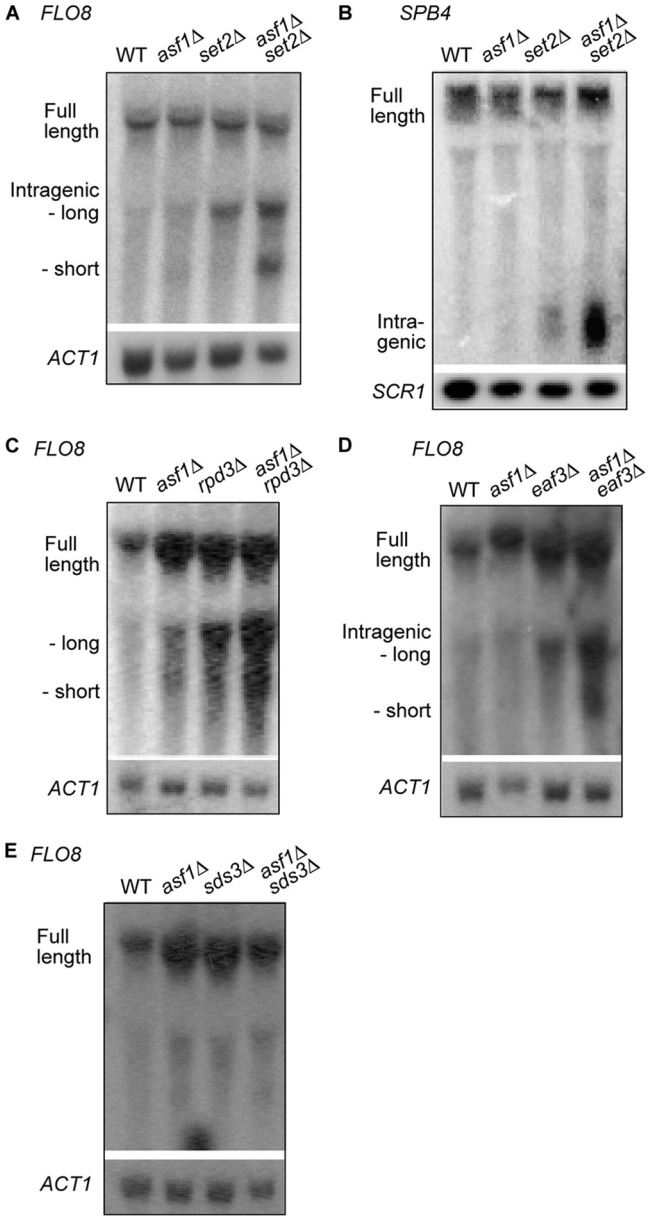

FIG. 4. Deletion of *ASF1* can exacerbate cryptic intragenic transcription in cells lacking Set2. (A to E) Northern blot analysis of transcripts arising from the *FLO8* and *SPB4* loci in the indicated strains. *ACT1* and *SCR1* are loading controls.

K36 methylation. In other words, Asf1 plays an important role in suppression of intragenic transcription when H3 cannot be methylated at K36.

The same is likely true at another gene, *SPB4*, where inactivation of *SPT6* is known to be associated with induction of a single spurious transcript (23). A tightly clustered population of abnormal *SPB4* transcripts also accumulates in cells lacking *SET2* (Fig. 4B). These transcripts are not induced in an *asf1*Δ single mutant but are very abundant in cells lacking both *ASF1* and *SET2*. Collectively, these results suggest that Asf1 and Set2 modulate spurious intragenic transcription in *FLO8* and *SPB4* as components of independent pathways.

This idea was supported by experiments in which we assessed the genetic interactions between *ASF1* and genes encoding components of the Rpd3S complex, whose role in suppression of intragenic transcription depends on Set2 (6, 24). Since Rpd3S is in the same pathway as Set2, its inactivation in *asf1*Δ cells is expected to have an additive effect on intragenic transcription similar to the effect of deleting *SET2*. Rpd3S was inactivated by deleting the gene encoding its catalytic subunit (*RPD3*). As predicted, spurious intragenic transcription at

FLO8 is more pronounced in *asf1*Δ *rpd3*Δ cells than in either single mutant (Fig. 4C). The Eaf3 subunit of Rpd3S is required for interaction of Rpd3S with Set2-methylated nucleosomes (31). Therefore, in *asf1*Δ cells, deletion of *EAF3* is also expected to have the same effect on spurious intragenic transcription as deletion of *SET2*. Figure 4D shows that spurious intragenic transcription at *FLO8* is indeed more pronounced in *asf1*Δ *eaf3*Δ cells than in either single mutant. Rpd3 exists in an additional complex (Rpd3L), which does not function in Set2-dependent chromatin deacetylation (6). Deletion of *SDS3*, which encodes a protein found in Rpd3L, but not Rpd3S, does not exacerbate spurious intragenic transcription in *asf1*Δ cells (Fig. 4E). We conclude that Asf1 functions separately from Set2 and Rpd3S in a pathway that affects suppression of spurious intragenic transcription at *FLO8*.

The latter conclusion was reinforced by a chromatin immunoprecipitation (ChIP) experiment in which we assessed H3 K36 di- and trimethylation at *FLO8* after correction for total H3 occupancy (Fig. 5A). As shown in Fig. 5B and C, deletion of *ASF1* has no effect on H3 K36 methylation at the 5′ or 3′ end of the coding region of *FLO8*.

On the basis of the known biochemical activities of Asf1, we hypothesized that its contribution to transcriptional regulation at *FLO8* depends on the conserved mechanism by which its core domain binds to the H3/H4 heterodimer (13, 35). Accordingly, we tested, using a genetic complementation approach, whether the capacity of Asf1 to bind to H3/H4 is important for suppression of spurious intragenic transcription in the coding region of *FLO8*. Mutation of valine 94 of Asf1 to arginine almost completely eliminates its histone binding activity (34). As expected, wild-type Asf1 expressed from a low-copy vector fully suppresses expression of the short intragenic transcript in *asf1*Δ *set2*Δ cells (Fig. 6A). Asf1^{V94R}, although expressed at the same level as the wild-type protein (Fig. 6B), fails to suppress this phenotype (Fig. 6A). Therefore, the ability of Asf1 to bind to H3/H4 is important for suppression of spurious intragenic transcription.

Since induction of cryptic intragenic transcription is associated with histone hyperacetylation (see the introduction) and Asf1 can inhibit H3/H4 acetylation (49), we reasoned that in the absence of *ASF1*, cryptic intragenic transcription may be increased in *FLO8* due to histone hyperacetylation. Analysis by ChIP, however, revealed that loss of Asf1 expression has little or no effect on H3 K9ac/K14ac in *FLO8* (Fig. 6C and D). H4 acetylation at the 5′ end of *FLO8* is also unaffected by deletion of *ASF1* (Fig. 6E). At the 3′ end of the coding region of *FLO8*, however, deletion of *ASF1* causes a substantial increase in H4 acetylation (Fig. 6F). This effect of *ASF1* deletion on H4 acetylation is additive with the induction of acetylation caused by *SET2* deletion. Therefore, Asf1 modulates H4 acetylation by a Set2-independent mechanism. Since bulk H3 cross-linking was not strongly affected by deletion of *ASF1* (Fig. 5A), overall our results indicate that Asf1 modulates spurious intragenic transcription at *FLO8* by a mechanism that affects H4 acetylation but is independent of the regulation of H3 K36 methylation by Set2.

Asf1 can contribute to the switch from di- to trimethylation of H3 K36. The data we obtained for *FLO8* and *SPB4* (Fig. 4) support the notion that Asf1 is not an essential component of a linear pathway of chromatin regulation that depends on Set2.

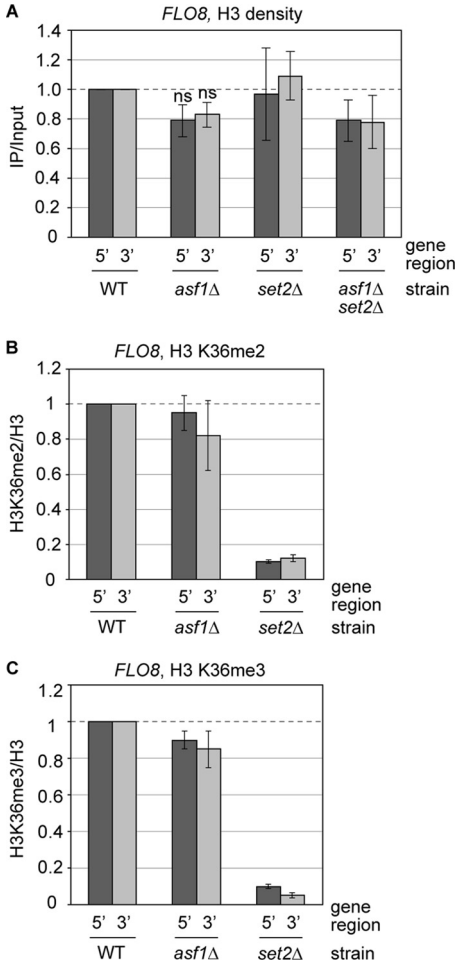

FIG. 5. Effect of *ASF1* deletion on di- and trimethylation of H3 K36 at *FLO8*. (A) Chromatin immunoprecipitation analysis of total H3 cross-linking to *FLO8* in wild-type, *asf1*Δ, *set2*Δ, and *asf1*Δ *set2*Δ strains (ns, not significant [$P > 0.05$]). (B and C) Cross-linking of dimethylated and trimethylated H3 K36 at the 5′ and 3′ ends of *FLO8* was assayed by ChIP in *asf1*Δ and *set2*Δ strains. Cross-linking in *set2*Δ cells reveals nonspecific H3 recovery by the anti-H3 K36me2/3 antibodies.

They do not, however, rule out the possibility that Asf1 and Set2 collaborate in chromatin regulation at these or other genes.

PMA1 is a frequently transcribed gene that is known to be occupied by Set2 (28, 57). In view of the evidence that Asf1 might modulate overall H3 K36 trimethylation by Set2 (Fig. 3C), we tested whether deletion of *ASF1* affects H3 K36me3 in the coding region of *PMA1* by ChIP (Fig. 7). Surprisingly, in contrast to *FLO8* (Fig. 5C), trimethylation of H3 K36 throughout the coding region of *PMA1* partly depends on Asf1 (Fig. 7A) (Fig. 7B shows the H3 cross-linking control). This dependency is not observed for H3 K36 dimethylation (Fig. 7C). These results suggest that Asf1 modulates the switch from di- to trimethylation of H3 K36.

Using ChIP, we also determined the effect of the Asf1 V94R mutation on H3 K36 trimethylation. Figure 7D shows that H3 K36 trimethylation in the coding region of *PMA1* is significantly impaired in the *asf1*^{V94R} mutant, as it is in the *ASF1* null

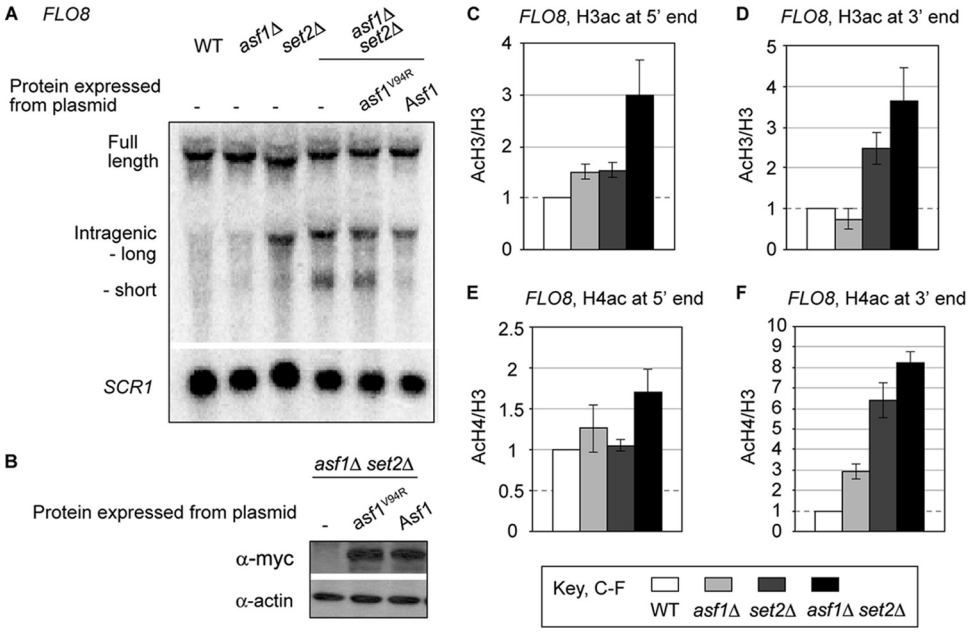

FIG. 6. (A) Asf1 suppresses cryptic intragenic transcription at *FLO8* by a mechanism that requires H3/H4 binding. Northern blotting was used to detect *FLO8* transcripts, and *SCR1* RNA serves as a loading control. (B) Immunoblot analysis of Asf1-myc and *asf1*^{V94R}-myc expression from pRS314. Actin serves as a loading control. (C to F) Deletion of *ASF1* and *SET2*, alone and in combination, can affect H3/H4 acetylation in the coding region of *FLO8*. Cross-linking of K9/K14-acetylated H3 and tail-acetylated H4 at the 5′ and 3′ ends of *FLO8*. The results shown are the means ± standard errors of the means (SEM) (error bars) from three independent experiments.

mutant (Fig. 7A). H3 cross-linking remains unaffected (Fig. 7E). We conclude that the ability of Asf1 to stimulate the switch from di- to trimethylation of H3 K36 in *PMA1* requires robust H3/H4 binding by Asf1.

The activity of Rtt109, the lysine acetylase (KAT) that acetylates K56 in the histone fold domain of H3, is known to depend on Asf1 (10, 20). Furthermore, Rtt109 activity is impaired by the Asf1 V94R mutation (21). These facts and the recent observation that H3 acetylated K56 (K56ac) has a strong destabilizing effect on nucleosomes (37) led us to hypothesize that mutation of *ASF1* may affect H3 K36me3 through an effect on H3 K56ac. To test this hypothesis, we asked whether H3 K36me3 in *PMA1* is misregulated in an *rtt109*Δ strain by using ChIP. It is not (Fig. 7F). Furthermore, we do not detect a synthetic sick interaction between *SET2* and *RTT109* in plating assays (Fig. 7G). Therefore, Asf1 does not modulate H3 K36me3 by virtue of an effect on acetylation at H3 K56.

Asf1 can contribute to gene localization of Set2. Asf1 could stimulate H3 K36 trimethylation in coding regions by multiple mechanisms. Two mechanisms that seem likely are (i) indirect stimulation of Set2 activity and (ii) direct enhancement of Set2 recruitment to target genes. We have not exhaustively explored possible indirect mechanisms for induction of Set2 activity in *asf1*Δ cells, because our data (below) suggest that Asf1 directly controls Set2 occupancy of *PMA1*.

We used ChIP to test whether Asf1 contributes to the association of Set2 with *PMA1*. As shown in Fig. 8A, Set2 cross-linking in the coding region of this gene is significantly dampened in *asf1*Δ cells. The converse is not true: using the ChIP assay validated in Fig. 8B, we find that cross-linking of Asf1 is unaffected by *SET2* deletion (Fig. 8C). Since deletion of *ASF1* does not inhibit the expression of Set2 (Fig. 3D and 8D), these findings are consistent with a direct role for Asf1 in promoting Set2 occupancy in the coding region of *PMA1*.

We tested whether the capacity of Asf1 to bind to the H3/H4 dimer is important for Set2 localization to *PMA1* by ChIP. Figure 8E shows that Set2 cross-linking to *PMA1* is impaired in cells that express Asf1^{V94R} in place of wild-type Asf1 (expression of relevant proteins in this experiment is shown in Fig. 8D). Therefore, H3/H4 binding by Asf1 is essential for normal Set2 association with *PMA1*.

Because a soluble complex that includes both Asf1 and Set2 has not been reported in the literature, it seems unlikely that these molecules are recruited to *PMA1* as components of a stable assemblage of proteins. Our ChIP results do not, however, rule out the possibility that interactions (possibly indirect) between Asf1 and Set2 contribute to Set2 cross-linking to genes such as *PMA1*. These interactions would likely be strong but short-lived or persistent but weak.

The notion that some functional interactions between Asf1 and Set2 could involve their direct or indirect physical association is supported by our analysis of Asf1-associated proteins obtained by tandem affinity purification (TAP). We isolated Asf1-TAP complexes and identified some of the species in this preparation by mass spectrometric analysis of trypsin-digested gel slices. Many proteins already known to associate with Asf1 were identified (Hir1, Hir2, Hir3, Rad53, Hpc2) (Fig. 9A) (12, 19, 22, 38). One gel slice also yielded a peptide that was assigned to Set2. This result suggested that Asf1 and Set2 coexist in a "rare" complex.

We further tested the hypothesis that Asf1 and Set2 can occur in the same complex by purifying Asf1- and Set2-TAP from strains that also expressed HA epitope-labeled Set2 (Set2-HA) or myc epitope-labeled Asf1 (Asf1-myc). We de-

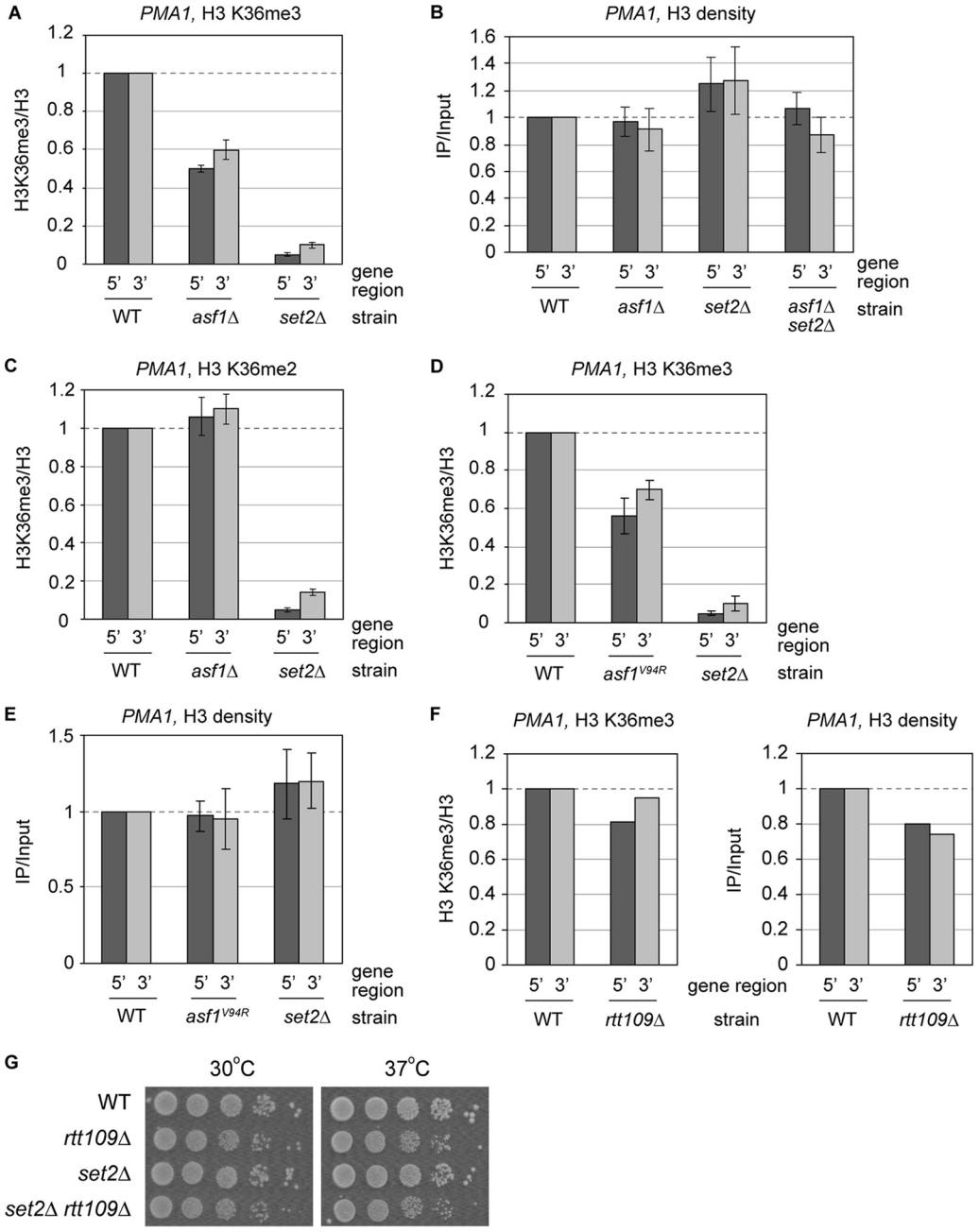

FIG. 7. Regulation of H3 K36 di- and trimethylation levels at *PMA1*. (A to C) Chromatin immunoprecipitation analysis of cross-linking of di- and trimethylated H3 K36 and bulk H3 at the 5′ and 3′ ends of *PMA1* in the indicated null mutants. (D and E) Cross-linking of trimethylated H3 K36 and bulk H3 at the 5′ and 3′ ends of *PMA1* was assayed by ChIP in cells expressing wild-type (WT) Asf1 or $asf1^{V94R}$. (F) Chromatin immunoprecipitation analysis of H3 K36me3 in wild-type and *rtt109*Δ strains. The data are normalized to H3 cross-linking. These results are the average values from two experiments. (G) Simultaneous deletion of *SET2* and *RTT109* does not confer a synthetic sick phenotype. Fivefold serial dilutions of cells were spotted onto YPD plates and photographed after 3 days of growth at 30 and 37°C.

tected Set2 in association with Asf1-TAP and Asf1 in association with Set2-TAP (Fig. 9B and C). In each case, the amount of HA- or myc-tagged protein in the final eluate represented only a very small fraction of the respective protein present in the input. This finding is consistent with cooccurrence of a subset of Asf1 and Set2 molecules in low-abundance protein complexes.

Trimethylation of H3 K36 by Set2 requires phosphorylation of the CTD of elongating RNAP II by protein kinase Ctk1 and phosphorylation of the domain of Set2 that is known to bind to RNAP II (59). It follows that if complexes containing Asf1 and Set2 form only on DNA, then their existence is likely to depend on expression of Ctk1. To test this possibility, we determined whether the recovery of Set2-HA in Asf1-TAP complexes is affected by deletion of *CTK1*. Despite the low expression of Set2 in *ctk1*Δ strains (59), Set2-HA was recovered in Asf1-TAP

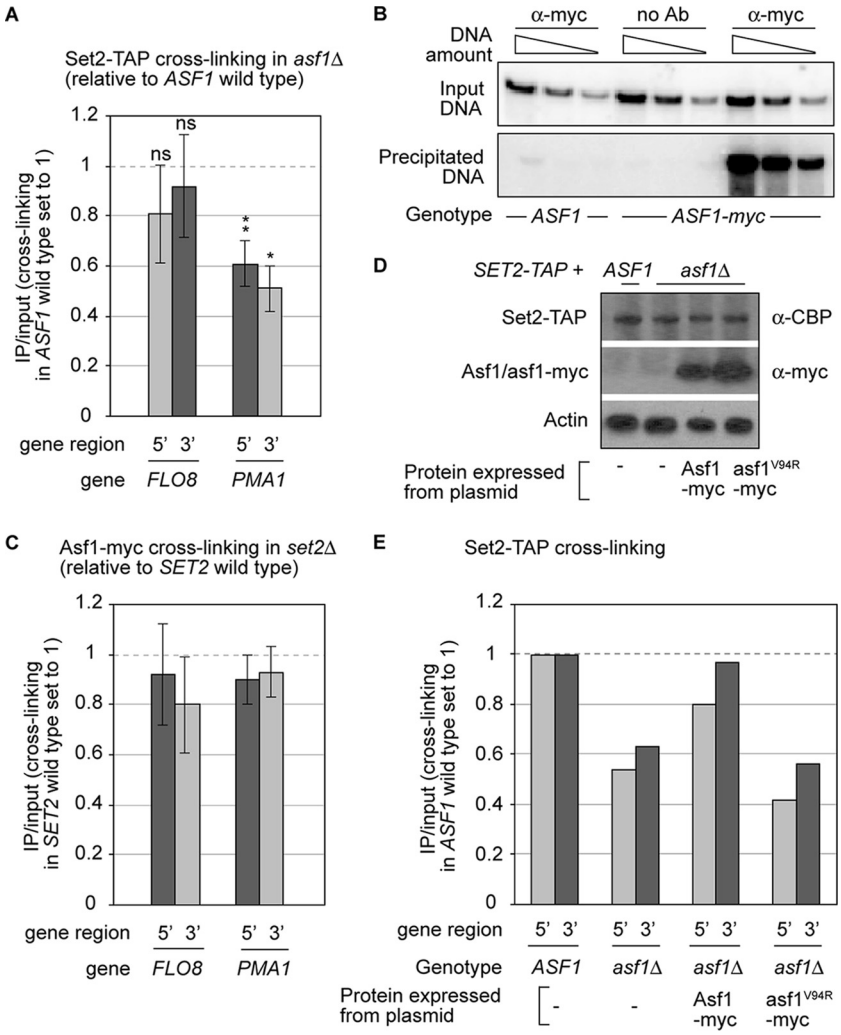

FIG. 8. Asf1 promotes association of Set2 with *PMA1*. (A) Set2 occupancy of the indicated genes in *asf1*Δ cells. Values that were not significantly different from the wild-type values (ns) and values that were significantly different from the wild-type values are indicated (*, $P = 0.009$; **, $P = 0.002$). (B) Validation of the ChIP assay for Asf1-myc. The experiment shows representative results of untagged Asf1 and no-antibody (no Ab) controls at the 3′ end of *PMA1*. (C) Asf1 occupancy in a *set2*Δ strain. The values represent the averages ± SEM from three experiments. (D) Immunoblotting analysis of Set2-TAP, Asf1-myc, and asf1^{V94R}-myc expressed from inserts in pRS316. Actin is the loading control. (E) Histone binding activity of Asf1 is required for Set2 localization at *PMA1*. Duplicate ChIP assays of SET2-TAP were performed in strains harboring empty vector (pRS316), pRS316 with *ASF1* as the insert, or pRS316 with *asf1^{V94R}* as the insert.

complexes obtained from a *CTK1* null mutant (Fig. 9D). We conclude that complexes that include Asf1 and Set2 can exist independently of Ctk1-phosphorylated RNAP II.

Misregulation of amino-terminal acetylation of H3 and H4 is associated with deletion of *ASF1* and *SET2*. In the context of our goal to gain a better overall appreciation of possible functional interplay between pathways of chromatin metabolism that depend on Asf1 and Set2, we further analyzed the effect of deleting *ASF1*, *SET2*, or both, on H3/H4 acetylation in the coding region of *PMA1*. These results are presented in Fig. 10A to D. Figure 10F summarizes the results of this experiment and of analysis of *FLO8* acetylation, which is shown in Fig. 6C to E.

Consistent with published evidence that Set2 promotes histone deacetylation (25, 46), deletion of *SET2*, when it has an effect, causes acetylation in coding regions to increase. In addition to the induction of H4 acetylation at the 3′ end of *FLO8* (Fig. 6F), deletion of *ASF1* is associated with increased H4 acetylation at the 5′ and 3′ ends of *PMA1* (Fig. 10A and B) and increased H3 acetylation at the 5′ end of *PMA1* (Fig. 10C). We conclude that Asf1 can inhibit tail acetylation of nucleosomal H3/H4 throughout coding regions. At the 3′ end of *PMA1* where Asf1 inhibits H4 acetylation, loss of Asf1 is associated with decreased H3 acetylation (Fig. 10D). Therefore, it appears that within a single region of a gene, Asf1 can stimulate H3 acetylation and inhibit H4 acetylation.

As noted in the introduction, Asf1 is a potential inhibitor of an H4 K16-specific KAT, the SAS complex (49). Increased H4 acetylation detected by ChIP using the pan-specific tetra-acetylated H4 antibody mixture (anti-K5ac/8ac/12ac/16ac) could be due to loss of this inhibition. To test this possibility, the effect of *ASF1* deletion specifically on H4 K16ac in *PMA1* was de-

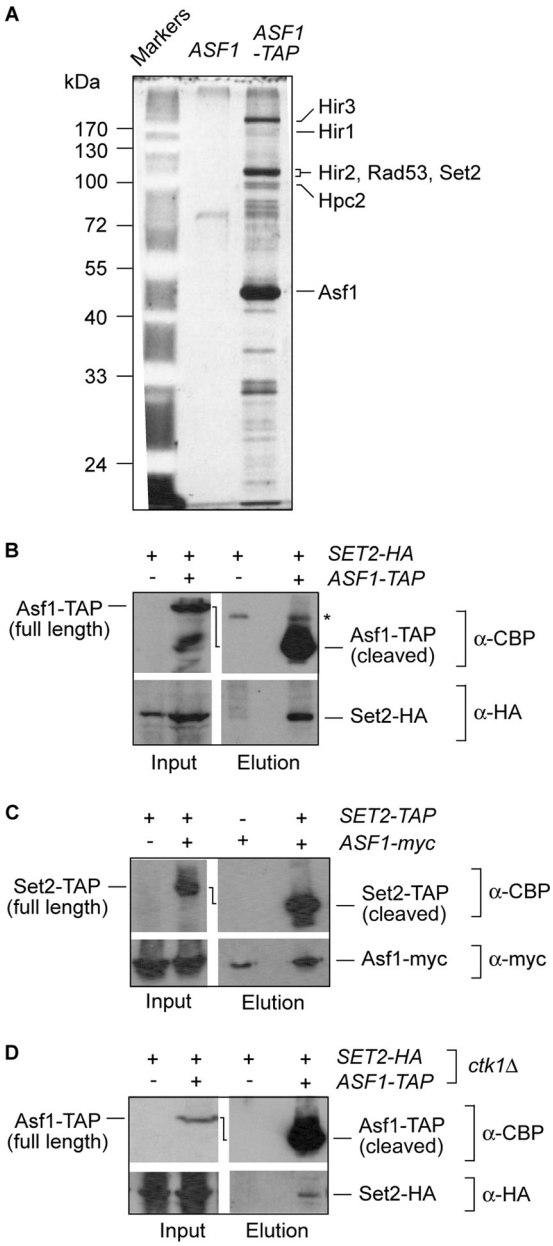

FIG. 9. (A to C) Set2 and Asf1 copurify. (A) Composition of protein complexes obtained by TAP from strains expressing untagged or TAP-tagged Asf1. Proteins in the TAP eluate were resolved by SDS-PAGE and detected by Sypro Ruby staining. Mass spectrometry was used to identify proteins in the Asf1-TAP sample. Most of the unlabeled bands were found to be ribosomal proteins. (B) Tandem affinity purification was performed using extracts from strains expressing Set2-HA or Set2-HA and Asf1-TAP. Immunoblots of proteins obtained by TAP were probed with either anti-CBP (α-CBP) or anti-HA (α-HA) antibodies to detect Asf1 and Set2, respectively. "Input" fractions were obtained before the binding to the first affinity column and represent 1/4,000 of the amount of starting protein. (C) Tandem affinity purification from strains expressing untagged or TAP-tagged Set2 and Asf1-myc (methods as in panel B). (D) Copurification of Set2 and Asf1 in a *ctk1*Δ strain. Tandem affinity purification from strains expressing untagged or TAP-tagged Asf1 and Set2-HA (methods as in panel B).

termined by ChIP. H4 K16 acetylation does not differ between wild-type and *asf1*Δ cells at either the 5′ or 3′ end of *PMA1* (Fig. 10E). Therefore, Asf1 regulates H4 acetylation in *PMA1* at sites other than those preferentially acted on by the Sas2 catalytic subunit of the SAS complex.

The general nature of interplay between gene products in the generation of a specific phenotype can often be inferred by comparing the effects of individual deletions and combined deletions of the genes of interest. The genetic interactions between *ASF1* and *SET2* suggest that Asf1 and Set2 can separately contribute to the regulation of H3/H4 acetylation. For H3, there is an additive stimulatory effect of *ASF1* and *SET2* deletion on acetylation at the 5′ ends of *FLO8* and *PMA1* (Fig. 6C and 10C). Deletion of *ASF1* and *SET2* also has an additive positive effect on H4 acetylation, but in this case, it occurs at the 3′ ends of *FLO8* and *PMA1* (Fig. 6F and 10B). We conclude that Asf1 and Set2 can separately inhibit H3/H4 acetylation. Considering these findings, it is intriguing that deletion of *ASF1* is associated with decreased H3 acetylation at the 3′ end of *PMA1* and that this phenotype is suppressed by deletion of *SET2* (Fig. 10D).

DISCUSSION

This study shows that chromatin regulation in the coding regions of genes can involve separate contributions of Asf1 and Set2 or collaboration of Asf1 and Set2. The collaboration between Asf1 and Set2 enhances trimethylation of H3 K36.

Asf1 and Set2 can function separately in suppression of spurious intragenic transcription at a weakly transcribed gene. Recent work by Youdell et al. (59) and Li et al. (32) revealed that Set2 dimethylation of H3 K36 is sufficient for suppression of intragenic transcription by the Rpd3S complex. Asf1 does not affect H3 K36 dimethylation in the coding region of *FLO8* (Fig. 5B) and therefore is unlikely to suppress spurious intragenic transcription as a component of the Set2 pathway. Consistent with this interpretation, we also observe the following. (i) Asf1 does not affect Set2 cross-linking in the coding region of *FLO8* (Fig. 8A). (ii) The function of Asf1 in transcription at *FLO8* is genetically separable from the functions of Set2 and components of the Rpd3S complex (Fig. 4 and 6A).

How does deletion of *ASF1* result in changes in H3/H4 acetylation state in coding regions? Deletion of *ASF1* is associated with decreased histone acetylation in some locations and increased acetylation in others (this study). If we take the evidence that Asf1 can directly stimulate H3 K56 acetylation by Rtt109 (10, 20) to indicate a more general ability for Asf1 to stimulate KAT reactions (for example, acetylation of other H3 residues), then decreased histone acetylation in *asf1*Δ cells is not surprising. However, the locus specificity of this effect remains unexplained (for example, Asf1 appears to stimulate H3 acetylation at the 3′ end of *PMA1* [Fig. 10D] but not at the 3′ end of *FLO8* [Fig. 6D]).

Our observation that deletion of *ASF1* is often associated with increased histone acetylation (for example, H4 at the 3′ end of *FLO8* and at the 5′ end of *PMA1*; Fig. 6F and 10A, respectively) suggests that in some contexts, Asf1 can inhibit acetylation. Asf1 can inhibit H4 K16 acetylation by the SAS complex *in vitro* (49), but this regulation is not important at the

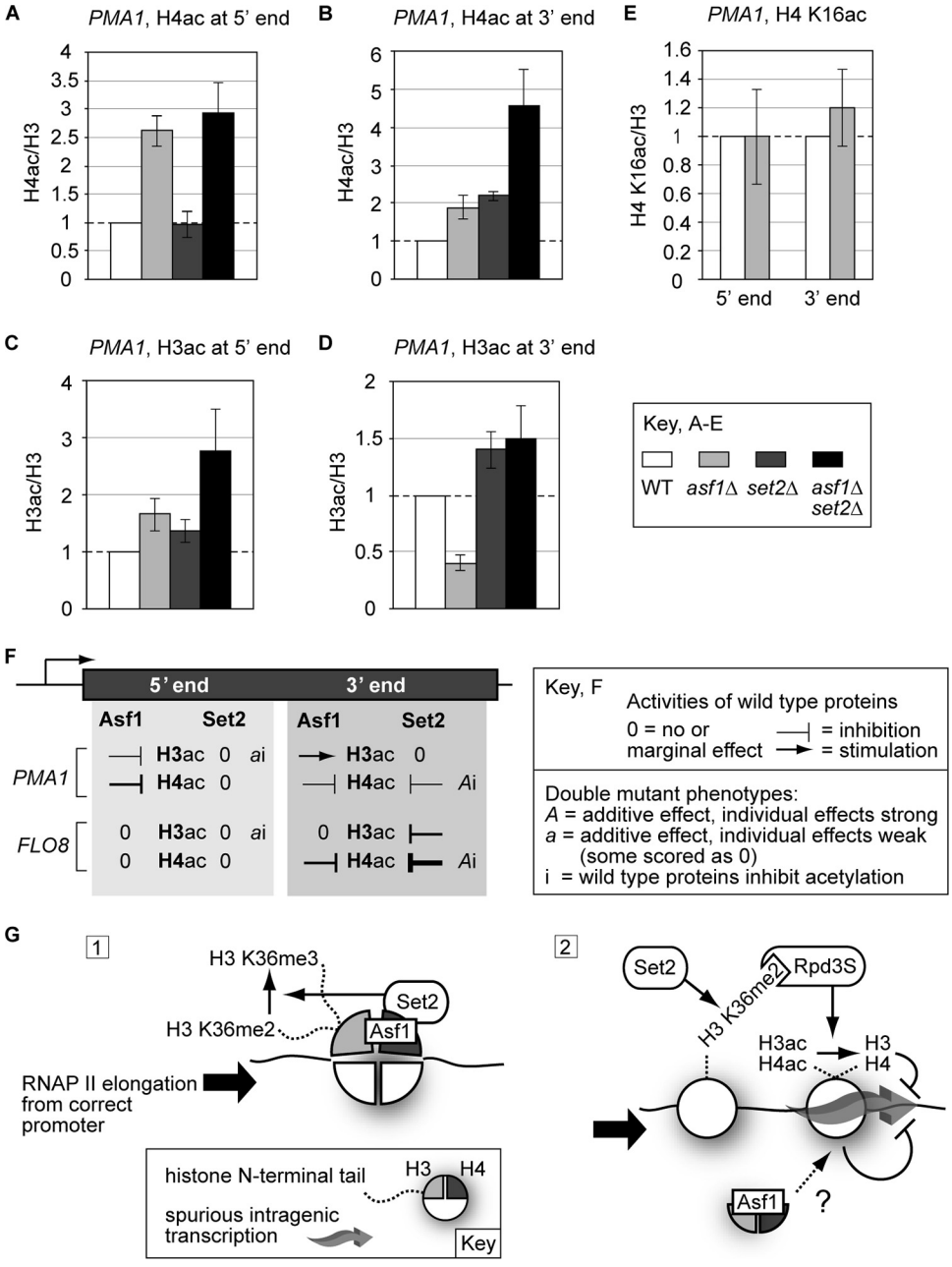

FIG. 10. (A to D) Chromatin immunoprecipitation analysis of H3 acetylation (K9 and K14) and H4 acetylation (K5, K8, K12, and K16) in the coding region of *PMA1* in wild-type, *asf1*Δ, *set2*Δ, and *asf1*Δ *set2*Δ strains. The graphs show the means ± SEM (error bars) for five independent experiments. (E) Chromatin immunoprecipitation analysis of H4 K16 acetylation in the coding region of *PMA1* in wild-type and *asf1*Δ strains. (F) Summary of the regulation of H3 and H4 acetylation at *PMA1* and *FLO8* inferred from our ChIP analysis. The arrows and T icons represent the stimulatory and inhibitory activities of wild-type proteins, respectively. (G) Speculative models of the Set2-dependent (diagram 1) and Set2-independent (diagram 2) functions of Asf1 in chromatin regulation. See text for details.

gene we studied because its H4 K16 acetylation state is unaffected by deletion of *ASF1* (Fig. 10E). An indirect mechanism could also account for increased histone acetylation in the absence of *ASF1*. For example, considering the finding that Asf1 inhibits spurious intragenic transcription in *FLO8* (7), a simple explanation for increased H4 acetylation at the 3′ end of this gene in *asf1*Δ cells (Fig. 6F) would be that hyperacetylation is caused by intragenic transcription. This model demands an explanation for increased intragenic transcription in *asf1*Δ cells. At this time, however, induction of cryptic transcription in *FLO8* as a result of loss of Asf1 expression is difficult to explain. Most importantly, although decreased nucleosome assembly activity could induce spurious transcription in the absence of Asf1, we observe little effect of *ASF1* deletion on H3 cross-linking in the coding region of *FLO8* (Fig. 5A).

Despite the wealth of published information about the regulation of histone acetylation (30, 43), at this time we cannot envisage a straightforward mechanism by which deletion of

ASF1 differentially stimulates H3 K9/K14 acetylation and inhibits H4 tail acetylation at the 3′ end of *PMA1* (Fig. 10B and D). Similarly, the locus-specific genetic interactions between *ASF1* and *SET2* summarized in Fig. 10F remain unexplained at a molecular level. We cannot rule out complex indirect effects by which the balance of KAT/HDAC activity toward H3 and H4 is differentially affected by deletion of *ASF1*.

Asf1 can promote the association of Set2 with chromatin and the switch from di- to trimethylation of H3 K36. The results of previous studies have not yet provided a robust understanding of the mechanism for specific association of Set2 with the coding regions of genes. A large body of early work supported the idea that the critical step in recruitment of Set2 to chromatin is its binding to the serine 2 phosphorylated form of the CTD of RNAP II (reviewed in reference 15). More recent results, however, strongly suggest that Set2 association with one well-studied gene (*STE11*) does not involve this mechanism (59). An alternative mechanism for Set2 association with *STE11* was not elucidated.

Our analysis of *PMA1* and data in the literature suggest that Asf1 can play an important role in Set2 association with the coding region of an active gene. First, deletion of *ASF1* is associated with decreased cross-linking of Set2 to *PMA1* (Fig. 8A). Second, an expected functional consequence of reduced Set2 cross-linking to *PMA1* is readily apparent in *asf1*Δ cells, namely, decreased H3 K36 trimethylation (Fig. 7A).

How might Asf1 stimulate Set2 association with *PMA1* and H3 K36 trimethylation in its coding region? Since H3 K36 trimethylation by Set2 requires the elongating form of RNAP II (59), it would be reasonable to ascribe Asf1 stimulation of H3 K36 trimethylation in *PMA1* to stimulation of RNAP II occupancy. This possibility seems unlikely, however, since loss of Asf1 does not cause lower RNAP II cross-linking in the coding region of *PMA1* (42) (our unpublished data). Nonetheless, it does seem reasonable to suppose that the effect of Asf1 on Set2 association with *PMA1* is mechanistically related to its stimulation of H3 K36 trimethylation. Under this assumption, recent work on the role of histone binding by Set2 suggests a plausible model for Set2 regulation by Asf1.

Du et al. demonstrated that di- and trimethylation of H3 K36 by Set2 depends on the ability of Set2 to bind to histone H4 (11). This binding occurs in a loop region between the α1 and α2 helices of the H4 histone fold domain, and the binding critically requires K44 within the loop. Since the C terminus of H2A surrounds the side chain of H4 K44 in nucleosomes, it was proposed that efficient interaction of Set2 with H4 could require removal of H2A-H2B dimers. Asf1 binds to H3-H4 dimers in a way that prevents H2A-H2B association and leaves the loop containing H4 K44 exposed (13, 35). We propose that the complex of Asf1 with a H3/H4 dimer could be a preferred substrate for H4 binding by Set2 (Fig. 10G, diagram 1). Two of our findings support this idea. First, the existence of a complex containing Asf1 and Set2 (albeit of very low abundance) is consistent with a reaction pathway involving the formation of an intermediate comprised of Asf1, H3/H4, and Set2. Second, Asf1 must be able to tightly bind to H3/H4 in order to stimulate Set2 association with *PMA1* and H3 K36 trimethylation (Fig. 7D and 8E). We envisage an overall model in which Asf1 stimulates H3 K36 trimethylation in the course of an elongation-coupled nucleosome reconfiguration cycle by transiently promoting H3/H4 association with Set2 (Fig. 10G, diagram 1). Reorganization of H2A/H2B dimers in nucleosomes, required for execution of this regulation, could be performed by the H2A/H2B chaperone FACT, which is known to function in the coding regions of transcribed genes (58).

In addition to functioning in a single pathway, Asf1 and Set2 have independent roles which impinge on chromatin in a way that suppresses spurious intragenic transcription. Importantly, Asf1 does not inhibit unwanted intragenic transcription as a component of the pathway which involves HDAC recruitment by Set2-dependent H3 K36 dimethylation (Fig. 10G, diagram 2). We know that suppression of intragenic transcription by Asf1 depends on its ability to bind to H3/H4, and therefore involves regulation of the nucleosome (Fig. 6A and Fig. 10G, diagram 2). The possibility that disruption of the latter regulation has indirect effects that induce spurious intragenic transcription in *ASF1* mutants remains to be investigated.

What is the function of H3 K36 trimethylation in yeast? Since H3 K36me3 is not necessary for suppression of spurious intragenic transcription (32, 59), it likely has other roles in chromatin regulation. One might be to control gene silencing by the Sir proteins (41). Set2 and H3 K36 methylation are known to antagonize silencing by a mechanism that does not involve suppression of spurious intragenic transcription (51). It follows that the ability of Asf1 to promote the switch from di- to trimethylation of H3 K36 might be important for control of silencing. In favor of this possibility is the evidence that silencing is modulated by Asf1 (29, 48). While H3 K36me3 might be important for silencing, it is unlikely that silencing-related functions of H3 K36me3 are relevant to its function at *PMA1*. We base this proposal on the finding that the nonconserved C-terminal domain of Asf1 contributes to the regulation of silencing (50) but is not needed for the H3 K36 dimethylation to trimethylation switch at *PMA1* (L. Lin, L. V. Minard, and M. C. Schultz, data not shown). Accordingly, we suspect that Asf1-dependent switching from di- to trimethylation of H3 K36 in *PMA1* has a role in the regulation of chromatin function not yet revealed by published studies of Set2.

ACKNOWLEDGMENTS

Darren Hockman is thanked for excellent technical assistance, and members of the Schultz lab are acknowledged for helpful discussions. We thank Carl Mann for plasmids.

This work was supported by grants to M.C.S. from the Canadian Institutes of Health Research and the Alberta Heritage Foundation for Medical Research and by grants to G.C.J. and R.A.S. from the Canadian Institutes of Health Research. L.L. was supported in part by a QEII Scholarship from the Government of Alberta, and L.V.M. was supported in part by a Master's Award from the Canadian Institutes for Health Research.

REFERENCES

1. **Adkins, M. W., J. J. Carson, C. M. English, C. J. Ramey, and J. K. Tyler.** 2007. The histone chaperone anti-silencing function 1 stimulates the acetylation of newly synthesized histone H3 in S-phase. J. Biol. Chem. **282:**1334–1340.
2. **Adkins, M. W., and J. K. Tyler.** 2004. The histone chaperone Asf1p mediates global chromatin disassembly in vivo. J. Biol. Chem. **279:**52069–52074.
3. **Aparicio, O., J. V. Geisberg, and K. Struhl.** 2004. Chromatin immunoprecipitation for determining the association of proteins with specific genomic sequences in vivo. *In* J. S. Bonifacino, M. Dasso, J. B. Harford, J. Lippincott-Schwartz, and K. M. Yamada (ed.), Current protocols in cell biology, chapter 17, unit 17.7. John Wiley and Sons, New York, NY.
4. **Biswas, D., R. Dutta-Biswas, D. Mitra, Y. Shibata, B. D. Strahl, T. Formosa, and D. J. Stillman.** 2006. Opposing roles for Set2 and yFACT in regulating TBP binding at promoters. EMBO J. **25:**4479–4489.

5. **Brachmann, C. B., A. Davies, G. J. Cost, E. Caputo, J. Li, P. Hieter, and J. D. Boeke.** 1998. Designer deletion strains derived from Saccharomyces cerevisiae S288C: a useful set of strains and plasmids for PCR-mediated gene disruption and other applications. Yeast **14:**115–132.
6. **Carrozza, M. J., B. Li, L. Florens, T. Suganuma, S. K. Swanson, K. K. Lee, W. J. Shia, S. Anderson, J. Yates, M. P. Washburn, and J. L. Workman.** 2005. Histone H3 methylation by Set2 directs deacetylation of coding regions by Rpd3S to suppress spurious intragenic transcription. Cell **123:**581–592.
7. **Cheung, V., G. Chua, N. N. Batada, C. R. Landry, S. W. Michnick, T. R. Hughes, and F. Winston.** 2008. Chromatin- and transcription-related factors repress transcription from within coding regions throughout the Saccharomyces cerevisiae genome. PLoS Biol. **6:**e277.
8. **Chu, Y., R. Simic, M. H. Warner, K. M. Arndt, and G. Prelich.** 2007. Regulation of histone modification and cryptic transcription by the Bur1 and Paf1 complexes. EMBO J. **26:**4646–4656.
9. **Collins, S. R., K. M. Miller, N. L. Maas, A. Roguev, J. Fillingham, C. S. Chu, M. Schuldiner, M. Gebbia, J. Recht, M. Shales, H. Ding, H. Xu, J. Han, K. Ingvarsdottir, B. Cheng, B. Andrews, C. Boone, S. L. Berger, P. Hieter, Z. Zhang, G. W. Brown, C. J. Ingles, A. Emili, C. D. Allis, D. P. Toczyski, J. S. Weissman, J. F. Greenblatt, and N. J. Krogan.** 2007. Functional dissection of protein complexes involved in yeast chromosome biology using a genetic interaction map. Nature **446:**806–810.
10. **Driscoll, R., A. Hudson, and S. P. Jackson.** 2007. Yeast Rtt109 promotes genome stability by acetylating histone H3 on lysine 56. Science **315:**649–652.
11. **Du, H. N., I. M. Fingerman, and S. D. Briggs.** 2008. Histone H3 K36 methylation is mediated by a trans-histone methylation pathway involving an interaction between Set2 and histone H4. Genes Dev. **22:**2786–2798.
12. **Emili, A., D. M. Schieltz, J. R. Yates III, and L. H. Hartwell.** 2001. Dynamic interaction of DNA damage checkpoint protein Rad53 with chromatin assembly factor Asf1. Mol. Cell **7:**13–20.
13. **English, C. M., M. W. Adkins, J. J. Carson, M. E. Churchill, and J. K. Tyler.** 2006. Structural basis for the histone chaperone activity of Asf1. Cell **127:** 495–508.
14. **Friis, R. M. N., B. P. Wu, S. N. Reinke, D. J. Hockman, B. D. Sykes, and M. C. Schultz.** 2009. A glycolytic burst drives glucose induction of global histone acetylation by picNuA4 and SAGA. Nucleic Acids Res. **37:**3969–3980.
15. **Fuchs, S. M., R. N. Laribee, and B. D. Strahl.** 2009. Protein modifications in transcription elongation. Biochim. Biophys. Acta **1789:**26–36.
16. **Garcia, B. A., S. B. Hake, R. L. Diaz, M. Kauer, S. A. Morris, J. Recht, J. Shabanowitz, N. Mishra, B. D. Strahl, C. D. Allis, and D. F. Hunt.** 2007. Organismal differences in post-translational modifications in histones H3 and H4. J. Biol. Chem. **282:**7641–7655.
17. **Ghaemmaghami, S., W. K. Huh, K. Bower, R. W. Howson, A. Belle, N. Dephoure, E. K. O'Shea, and J. S. Weissman.** 2003. Global analysis of protein expression in yeast. Nature **425:**737–741.
18. **Goldstein, A. L., and J. H. McCusker.** 1999. Three new dominant drug resistance cassettes for gene disruption in Saccharomyces cerevisiae. Yeast **15:**1541–1553.
19. **Green, E. M., A. J. Antczak, A. O. Bailey, A. A. Franco, K. J. Wu, J. R. Yates III, and P. D. Kaufman.** 2005. Replication-independent histone deposition by the HIR complex and Asf1. Curr. Biol. **15:**2044–2049.
20. **Han, J., H. Zhou, B. Horazdovsky, K. Zhang, R. M. Xu, and Z. Zhang.** 2007. Rtt109 acetylates histone H3 lysine 56 and functions in DNA replication. Science **315:**653–655.
21. **Han, J., H. Zhou, Z. Li, R. M. Xu, and Z. Zhang.** 2007. Acetylation of lysine 56 of histone H3 catalyzed by RTT109 and regulated by ASF1 is required for replisome integrity. J. Biol. Chem. **282:**28587–28596.
22. **Hu, F., A. A. Alcasabas, and S. J. Elledge.** 2001. Asf1 links Rad53 to control of chromatin assembly. Genes Dev. **15:**1061–1066.
23. **Kaplan, C. D., L. Laprade, and F. Winston.** 2003. Transcription elongation factors repress transcription initiation from cryptic sites. Science **301:**1096–1099.
24. **Keogh, M. C., S. K. Kurdistani, S. A. Morris, S. H. Ahn, V. Podolny, S. R. Collins, M. Schuldiner, K. Chin, T. Punna, N. J. Thompson, C. Boone, A. Emili, J. S. Weissman, T. R. Hughes, B. D. Strahl, M. Grunstein, J. F. Greenblatt, S. Buratowski, and N. J. Krogan.** 2005. Cotranscriptional Set2 methylation of histone H3 lysine 36 recruits a repressive Rpd3 complex. Cell **123:**593–605.
25. **Kim, T., and S. Buratowski.** 2009. Dimethylation of H3K4 by Set1 recruits the Set3 histone deacetylase complex to 5′ transcribed regions. Cell **137:**259–272.
26. **Kizer, K. O., H. P. Phatnani, Y. Shibata, H. Hall, A. L. Greenleaf, and B. D. Strahl.** 2005. A novel domain in Set2 mediates RNA polymerase II interaction and couples histone H3 K36 methylation with transcript elongation. Mol. Cell. Biol. **25:**3305–3316.
27. **Kobor, M. S., S. Venkatasubrahmanyam, M. D. Meneghini, J. W. Gin, J. L. Jennings, A. J. Link, H. D. Madhani, and J. Rine.** 2004. A protein complex containing the conserved Swi2/Snf2-related ATPase Swr1p deposits histone variant H2A.Z into euchromatin. PLoS Biol. **2:**E131.
28. **Krogan, N. J., M. Kim, A. Tong, A. Golshani, G. Cagney, V. Canadien, D. P. Richards, B. K. Beattie, A. Emili, C. Boone, A. Shilatifard, S. Buratowski, and J. Greenblatt.** 2003. Methylation of histone H3 by Set2 in Saccharomyces cerevisiae is linked to transcriptional elongation by RNA polymerase II. Mol. Cell. Biol. **23:**4207–4218.
29. **Le, S., C. Davis, J. B. Konopka, and R. Sternglanz.** 1997. Two new S-phase-specific genes from Saccharomyces cerevisiae. Yeast **13:**1029–1042.
30. **Lee, K. K., and J. L. Workman.** 2007. Histone acetyltransferase complexes: one size doesn't fit all. Nat. Rev. Mol. Cell Biol. **8:**284–295.
31. **Li, B., M. Gogol, M. Carey, D. Lee, C. Seidel, and J. L. Workman.** 2007. Combined action of PHD and chromo domains directs the Rpd3S HDAC to transcribed chromatin. Science **316:**1050–1054.
32. **Li, B., J. Jackson, M. D. Simon, B. Fleharty, M. Gogol, C. Seidel, J. L. Workman, and A. Shilatifard.** 2009. Histone H3 lysine 36 dimethylation (H3K36me2) is sufficient to recruit the Rpd3s histone deacetylase complex and to repress spurious transcription. J. Biol. Chem. **284:**7970–7976.
33. **Longtine, M. S., A. McKenzie III, D. J. Demarini, N. G. Shah, A. Wach, A. Brachat, P. Philippsen, and J. R. Pringle.** 1998. Additional modules for versatile and economical PCR-based gene deletion and modification in Saccharomyces cerevisiae. Yeast **14:**953–961.
34. **Mousson, F., A. Lautrette, J. Y. Thuret, M. Agez, R. Courbeyrette, B. Amigues, E. Becker, J. M. Neumann, R. Guerois, C. Mann, and F. Ochsenbein.** 2005. Structural basis for the interaction of Asf1 with histone H3 and its functional implications. Proc. Natl. Acad. Sci. U. S. A. **102:**5975–5980.
35. **Natsume, R., M. Eitoku, Y. Akai, N. Sano, M. Horikoshi, and T. Senda.** 2007. Structure and function of the histone chaperone CIA/ASF1 complexed with histones H3 and H4. Nature **446:**338–341.
36. **Nelson, C. J., H. Santos-Rosa, and T. Kouzarides.** 2006. Proline isomerization of histone H3 regulates lysine methylation and gene expression. Cell **126:**905–916.
37. **Neumann, H., S. M. Hancock, R. Buning, A. Routh, L. Chapman, J. Somers, T. Owen-Hughes, J. van Noort, D. Rhodes, and J. W. Chin.** 2009. A method for genetically installing site-specific acetylation in recombinant histones defines the effects of H3 K56 acetylation. Mol. Cell **36:**153–163.
38. **Prochasson, P., L. Florens, S. K. Swanson, M. P. Washburn, and J. L. Workman.** 2005. The HIR corepressor complex binds to nucleosomes generating a distinct protein/DNA complex resistant to remodeling by SWI/SNF. Genes Dev. **19:**2534–2539.
39. **Ramaswamy, V., J. S. Williams, K. M. Robinson, R. L. Sopko, and M. C. Schultz.** 2003. Global control of histone modification by the anaphase-promoting complex. Mol. Cell. Biol. **23:**9136–9149.
40. **Riles, L., R. J. Shaw, M. Johnston, and D. Reines.** 2004. Large-scale screening of yeast mutants for sensitivity to the IMP dehydrogenase inhibitor 6-azauracil. Yeast **21:**241–248.
41. **Rusche, L. N., A. L. Kirchmaier, and J. Rine.** 2003. The establishment, inheritance, and function of silenced chromatin in Saccharomyces cerevisiae. Annu. Rev. Biochem. **72:**481–516.
42. **Schwabish, M. A., and K. Struhl.** 2006. Asf1 mediates histone eviction and deposition during elongation by RNA polymerase II. Mol. Cell **22:**415–422.
43. **Shahbazian, M. D., and M. Grunstein.** 2007. Functions of site-specific histone acetylation and deacetylation. Annu. Rev. Biochem. **76:**75–100.
44. **Sharp, J. A., E. T. Fouts, D. C. Krawitz, and P. D. Kaufman.** 2001. Yeast histone deposition protein Asf1p requires Hir proteins and PCNA for heterochromatic silencing. Curr. Biol. **11:**463–473.
45. **Sikorski, R. S., and P. Hieter.** 1989. A system of shuttle vectors and yeast host strains designed for efficient manipulation of DNA in Saccharomyces cerevisiae. Genetics **122:**19–27.
46. **Strahl, B. D., and C. D. Allis.** 2000. The language of covalent histone modifications. Nature **403:**41–45.
47. **Strahl, B. D., P. A. Grant, S. D. Briggs, Z. W. Sun, J. R. Bone, J. A. Caldwell, S. Mollah, R. G. Cook, J. Shabanowitz, D. F. Hunt, and C. D. Allis.** 2002. Set2 is a nucleosomal histone H3-selective methyltransferase that mediates transcriptional repression. Mol. Cell. Biol. **22:**1298–1306.
48. **Sutton, A., J. Bucaria, M. A. Osley, and R. Sternglanz.** 2001. Yeast ASF1 protein is required for cell cycle regulation of histone gene transcription. Genetics **158:**587–596.
49. **Sutton, A., W. J. Shia, D. Band, P. D. Kaufman, S. Osada, J. L. Workman, and R. Sternglanz.** 2003. Sas4 and Sas5 are required for the histone acetyltransferase activity of Sas2 in the SAS complex. J. Biol. Chem. **278:**16887–16892.
50. **Tamburini, B. A., J. J. Carson, J. G. Linger, and J. K. Tyler.** 2006. Dominant mutants of the Saccharomyces cerevisiae ASF1 histone chaperone bypass the need for CAF-1 in transcriptional silencing by altering histone and Sir protein recruitment. Genetics **173:**599–610.
51. **Tompa, R., and H. D. Madhani.** 2007. Histone H3 lysine 36 methylation antagonizes silencing in Saccharomyces cerevisiae independently of the Rpd3S histone deacetylase complex. Genetics **175:**585–593.
52. **Tong, A. H., M. Evangelista, A. B. Parsons, H. Xu, G. D. Bader, N. Page, M. Robinson, S. Raghibizadeh, C. W. Hogue, H. Bussey, B. Andrews, M. Tyers, and C. Boone.** 2001. Systematic genetic analysis with ordered arrays of yeast deletion mutants. Science **294:**2364–2368.
53. **Treco, D. A., and V. Lundblad.** 1993. Basic techniques of yeast genetics, p.13.1.1–13.1.7. *In* F. M. Ausubel, R. Brent, R. E. Kingston, D. D. Moore,

J. G. Seidman, J. A. Smith, and K. Struhl (ed.), Current protocols in molecular biology, vol. 2. John Wiley and Sons, New York, NY.

54. **Tyler, J. K., C. R. Adams, S. R. Chen, R. Kobayashi, R. T. Kamakaka, and J. T. Kadonaga.** 1999. The RCAF complex mediates chromatin assembly during DNA replication and repair. Nature **402:**555–560.
55. **Williams, S. K., D. Truong, and J. K. Tyler.** 2008. Acetylation in the globular core of histone H3 on lysine-56 promotes chromatin disassembly during transcriptional activation. Proc. Natl. Acad. Sci. U. S. A. **105:**9000–9005.
56. **Winzeler, E. A., D. D. Shoemaker, A. Astromoff, H. Liang, K. Anderson, B. Andre, R. Bangham, R. Benito, J. D. Boeke, H. Bussey, A. M. Chu, C. Connelly, K. Davis, F. Dietrich, S. W. Dow, M. El Bakkoury, F. Foury, S. H. Friend, E. Gentalen, G. Giaever, J. H. Hegemann, T. Jones, M. Laub, H. Liao, R. W. Davis, et al.** 1999. Functional characterization of the S. cerevisiae genome by gene deletion and parallel analysis. Science **285:**901–906.
57. **Xiao, T., H. Hall, K. O. Kizer, Y. Shibata, M. C. Hall, C. H. Borchers, and B. D. Strahl.** 2003. Phosphorylation of RNA polymerase II CTD regulates H3 methylation in yeast. Genes Dev. **17:**654–663.
58. **Xin, H., S. Takahata, M. Blanksma, L. McCullough, D. J. Stillman, and T. Formosa.** 2009. yFACT induces global accessibility of nucleosomal DNA without H2A-H2B displacement. Mol. Cell **35:**365–376.
59. **Youdell, M. L., K. O. Kizer, E. Kisseleva-Romanova, S. M. Fuchs, E. Duro, B. D. Strahl, and J. Mellor.** 2008. Roles for Ctk1 and Spt6 in regulating the different methylation states of histone H3 lysine 36. Mol. Cell. Biol. **28:**4915–4926.